High Performance Discharges in the HT-7 and HL-1M Tokamaks

Jiangang Li 1), Baonian Wan 1), Jiarong.Luo 1), Yanping Zhao 1), Xiaodong Zhang 1), Junyu Zhao 1), Fukun Liu 1), Xuemao Guo 1), Guangli Kuang 1), Yuejiang Shi 1), HT-7 team 1),

Yong Liu 2), Xuantong Ding 2), Lianghua Yao 2), Yi Liu 2), Jiafu Dong 2), Jung Riao 2), Zhen Feng 2), Enyao Wang 2), HL-1M Group 2)

1) Institute of Plasma Physics, Chinese Academy of Sciences, Hefei, China
2) Southwestern Institute of Physics, Chengdu, Sichuan, China

e-mail contact of main author: j_li@mail.ipp.ac.cn

Abstract: Significant progress in obtaining high performance discharges under a quasi-steady-state condition in the HT-7 super conducting tokamak has been realized since the last IAEA meeting. HT-7 has produced a variety of discharges with $\beta_N*H_{89} > 1$-4 for a duration of several to several tens of energy confinement times with a non-inductive driven current of 50-80%. The duration at $H_{89} > 1.5$ with $\beta_N \sim 1$ has been extended to 130 energy confinement times. A reproducible long pulse discharge with $T_e \sim 1$ keV and central density ~ $1x10^{19}m^{-3}$ can be easily obtained with a duration of 10-20 seconds. In the HL-1M tokamak, a kinetic MHD instability during ECRH and combined ECRH and LHCD was observed. This instability was driven purely by energetic electrons. By using high-pressure supersonic molecular beam injection, very high density and evidence of the onset of clustering were obtained.

1. High Performance Discharges in the HT-7 Superconducting Tokamak

1.1 .Introduction

An advanced tokamak operation mode under a steady-state condition of the tokamak plasma is one of the basic requirements for fusion reactors. A high confinement, high β plasma and instability stabilization are needed to meet this requirement for obtaining high performance regimes. The control of current density, pressure profile, and rotation profile is an important issue to attain both an internal transport barrier (ITB) for confinement enhancement and a high bootstrap current fraction with suitable additional non-inductive means for real steady-state operation. Efforts made in HT-7 tokamak experiments are contributing to these fusion reactor relevant issues and the underlying physics. Significant progress in obtaining high performance discharges under a quasi-steady state condition in the HT-7 tokamak has been realized since the last IAEA meeting. HT-7 has produced a variety of discharges with the normalized performance $\beta_N*H_{89} > 1$-4 for a duration of several to several tens of energy confinement times with a non-inductive driven current of 50-80%. Several important technical modifications have been made in the last two years [1]. The previous Mo limiter has been replaced by a full poloidal water cooled graphite limiter,

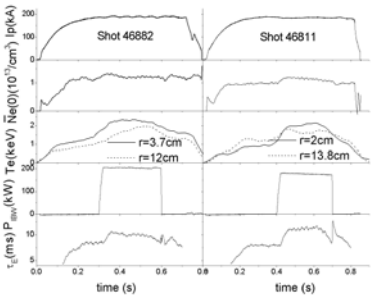

Fig. 1 Shot 46882, global electron heating, r(Ω_H) = 3cm, Shot 46811, local electron heating, at r (Ω_H) = 15.8 cm.

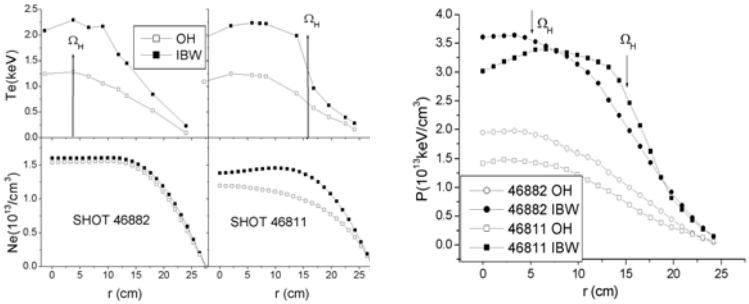

Fig. 2 Shots 46882 and 46811, T_e, n_e and electron pressure profiles in ohmic and IBW heating phase.

which increases the heat flux removal capability and reduces the influx of metal impurities for long pulse discharges. By a method of CVR, all carbon tiles were coated with above 100μm SiC gradient film to reduce the chemical sputtering and suppress the radiation-enhanced sublimation. The particle exhaust capability was increased by improved cryogenic pumping in the limiter area. Ferritic steel boards are installed in the vacuum chamber to reduce the ripples from 4.2% to 1.6% at the limiter radius on the low field side. LHCD and ICRF systems of 1.2 MW and 1.5MW, respectively, including power supply and launcher have been upgraded to CW operation mode.

1.2. Heating and Profile Control by IBW [2,3]

The IBW is attractive for fusion plasma heating because it has good accessibility to couple the power to the ion cyclotron resonant layer in the fusion plasma center. The $n_{||}$ spectrum of the IBW antenna in HT-7 is peaked at 8 for a frequency of 27 MHz, which is favorable for electron heating. The electron-heating mode for IBW was used in HT-7 for most cases. In the electron heating mode, the RF frequency was 27 MHz and the toroidal field strength was 1.8~2 T. Both global and localized electron heating was obtained depending on the location of the resonant layer in the plasma. Figure.1 shows typical results of global (shot 46822) and localized (46811) electron heating. The corresponding spatial profiles of electron temperature and density are shown in Fig. 2 for the target plasma and IBW heated phase. For shot 46822, the toroidal field strength was 1.85 T. The Ω_D or $2\Omega_H$ ion cyclotron resonant layer was located at a radius of 3.4 cm in the plasma center. The plasma current was 190 kA with $T_e(0) \sim 1.2$ keV and $\bar{n}_e(0) \sim 1.1\times10^{13}/cm^3$ in the pre-heated phase. During IBW injection, the global $T_e(r)$ was increased to $T_e(0) \sim 2.3$ keV, but was slightly peaked compared with the T_e profile in the target plasma. The electron density was kept almost unchanged. The global electron pressure profile shown in Fig. 2 was peaked during IBW in the global heating mode.

In shot 46811, the $2\Omega_D$ resonant layer is near the half plasma radius for the off-axis heating, corresponding to a toroidal magnetic field strength of 2 T. The electron temperature at half radius exceeded the central electron temperature after IBW was applied. The IBW absorption via ELD due to the $n_{||}$ spectrum is not dominant in this case because of the lower electron temperature in the outer half plasma region. The large increase of T_e around the resonant layer is a result of enhanced ELD because of the reduced wave group velocity. The

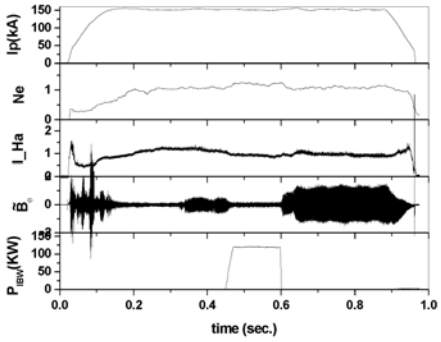

Fig. 3 MHD stabilization by IBW r(Ω_H) near the m=2/n=1 rational surface.

remaining IBW power available for the plasma ions can induce a ponderomotive sheared flow [4], which absorbs the particles toward the resonant layer. The central line averaged electron density is slightly increased during the IBW heated phase. This increase of density is mainly from the density increase around the resonant layer as shown in Fig. 2 for the density profiles, which resulted in a slightly broadened electron density profile. As a result, the local electron pressure profile was steep at the region around the resonant layer in the off-axis heating mode shown in Fig. 2. In both global and localized heating mode, the energy confinement was improved. But the effect was stronger in the localized heating mode, which may be a result of an extended high performance volume. A reduction of electron heat transport has been observed from sawtooth heat pulse propagation, which is consistent with the improved energy confinement.

In HT-7, the most dangerous MHD instability is m/n=2/1 resistive tearing mode, which is driven by the plasma current density gradient. The locked mode often leads to disruption in high power heated plasmas. IBW off-axis heating near the q=m/n=2/1 rational surface can modify the pressure profiles and then impact on MHD activity. A typical result is shown in Fig. 3. In this experiment, a frequency of 27 MHz is selected. The experimental results show that the electron pressure gradients are obviously reduced near the q=2 rational surface during IBW heating. Thus current density may be redistributed, which results in partial or complete MHD stabilization.

1.3. LHCD Experiments [5,6]

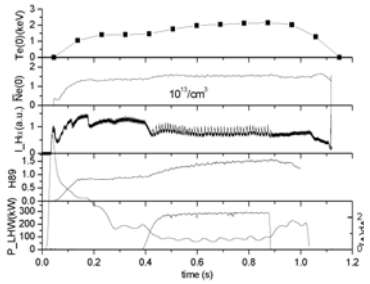

Fig. 4 An off-axis LHCD improved confinement shot.

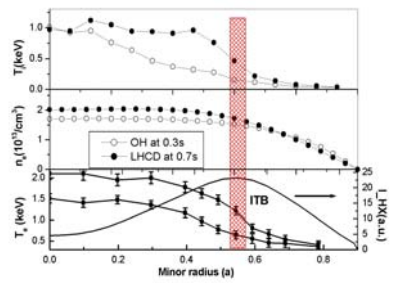

Fig. 5 T_i, T_e, n_e and HXR profiles for Fig. 4

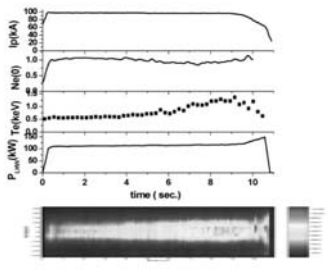

Fig. 6 A long pulse LHCD discharge with H_{89} close to unity. The bottom figure is the HXR profile.

Off-axis LHCD can be explored not only to sustain the plasma current, but also to control the profile of plasma current density and enhance the confinement. By proper optimization of LHCD launched spectra, plasma parameters and toroidal magnetic field, a high performance plasma can be achieved with an ITB-like profile of electron temperature and density. Figure 4 shows such a plasma discharge obtained by using LHCD. The plasma loop voltage dropped from 1.5 V in the ohmic phase to ~0.5 V after LHW was applied. The particle confinement is improved as indicated by increased electron density and decreased D_α radiation. The energy confinement was also improved. The corresponding H_{89} factor was 1.5 in the LHCD phase, meaning an improved performance. The profiles of electron/ion temperatures and density are given in Fig. 5. T_e, T_i and n_e are increased considerably and their profiles become broadened, which shows an ITB-like structure at r ~ 0.55a. The profile of the HX radiation during LHCD is also shown in Fig. 5. Its peak was located at the same position. To a first approximation, the HXR profile is an indicator of the fast electron current density driven by LHW. The simulated LHW power deposition profile using a ray tracing code with the parameters shown in the LHCD phase is nearly consistent with the HXR profile [5]. This fact suggests the importance of fast electron current density in plasma performance.

In the case of lower plasma parameters and lower performance with $H_{89} \geq 1$, the LHW power was deposited in the radial region closer to the plasma center. The plasma profiles were not as broad as in the cases with higher plasma parameters. Discharges can be sustained for up to several hundred τ_E and several τ_R. Figure 6 shows such a discharge for 10 s, which is about $1000\tau_E$ and $> 4\tau_R$. The factor of H_{89} was around unity for most of the discharge, meaning a good confinement. The HXR profile shown in the bottom part of the figure became broadened from ~3.5 s, which exceeds the current relaxation time, while the central electron temperature was slowly increased. Presently, it is not clear that the broadened fast electron current density was the result of increased T_e or current relaxation due to fast electron diffusion.

1.4. Synergy between LHW and IBW [7]

Recently, a theory was developed to interpret the IBW+LHW local synergy and to simulate the behavior of both waves in the PBX-M and FTU plasmas [8 and references therein]. The results found that IBW can modify the electron distribution function around maximum $n_{||}(x)$ and enhance localized damping of LHW. On another hand, features of off-axis heating by IBW are potentially capable of enhancing the LHCD plasma performance through extension of the high performance volume via LHW and IBW synergy. Figure 7 shows such an LHCD discharge with IBW of 27 MHz injection at a toroidal field strength of 2 T and plasma current of 200 kA with $N_{||}^{peak} = 2.3$. The corresponding ion cyclotron resonant layer is located at 0.5a. The central line averaged electron density and temperature were increased when IBW was applied. The electron density profile was broadened as shown by a decrease of $\bar{n}_e(0)/\bar{n}_e(10)$ during IBW. Compared with those in the LHW target plasma, the volume of high electron pressure was extended considerably as shown in Fig. 8. The largest gradient of electron pressure was located near the resonant layer. As a result of the above, the performance was significantly enhanced.

The HXR profiles are shown in Fig. 9 from a combined LHCD and IBW heated plasma. The HRX peak position was at 0.2a in the LHCD phase and stabilized at around 0.5a in the

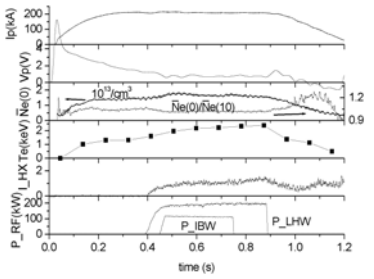

Fig. 7 Shot 46348, an LHCD + IBW discharge.

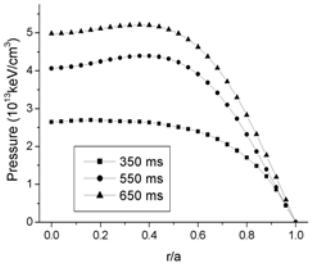

Fig. 8 Electron pressure profiles in the same condition as in Fig. 7.

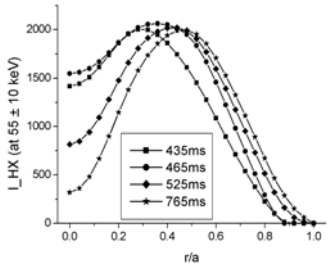

Fig. 9 HXR profiles for shot 46348.

two wave case. Most of the LHW power was absorbed in the region around 0.5a. This is coincident with the effect of the localized IBW heating, so that the LHCD driven efficiency is significantly increased in this region. IBW can act strongly with electrons via ELD near the resonant layer because of reduced phase velocity, and cause strong modification of the electron distribution function [8]. The peak in $I_{HX}(r)$ in an LHCD and IBW heated plasma is correlatedwith the region around the resonant layer, implying that the incoming LHWs can damp on the tail of the modified electron distribution function due to IBW injection and create localized current channels [8]. This feature can be utilized for an external control of current density and electron pressure profiles and hence for an integrated high performance.

1.5. Integrated High Performance under Steady-state Conditions

The features of IBW and LHCD are integrated to obtain long pulse high performance discharges. By proper optimization of operation, in particular by choosing a strategy to avoid MHD activity, high performance discharges under a quasi-steady-state condition in HT-7 have been realized under a very good wall condition with a very low impurity level (Z_{eff}<1.5) and low recycling, which is realized by intensive RF boronization. A variety of high performance discharge indicated by a normalized product β_N*H_{89} =1-4 was produced for a duration of several tens to hundreds of energy confinement times.

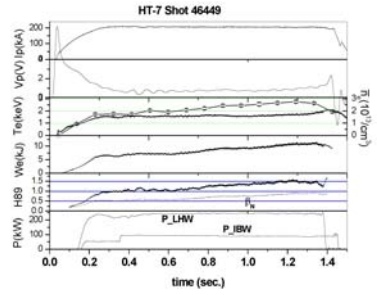

Fig.10. High performance with maximum $T_e(0)$~3 keV, H_{89} >1.

Figure 10 shows such an optimized discharge obtained by utilizing synergy between LHW and IBW. In this shot, the plasma current was 200 kA, B_T = 2 T and the central line averaged density was $1.6\times10^{13}/cm^3$. The highest electron temperature was $T_e(0)$ ~ 3 keV. The performance indicated by the H_{89} factor exceeded unity for 1.2 s, which was about $50\tau_E$ for averaged energy confinement time, but normalized β_N was still low and below unity for most of the discharge due to higher I_p and B_T. The normalized plasma performance indicated by β_N*H_{89} >3 and H_{93} ~ 1.5 was achieved (Fig. 11) for >$50\tau_E$ with I_p ~ 130 kA and B_T = 1.85 T. The resonant layer of IBW with a frequency of 27 MHz was at about r=3 cm, very close to the plasma center. The first maximum of $n_{||}$ was located around 15 cm (0.55a). The profiles of electron temperature and density were gradually broadened in the plasma core region up to about half the minor radius. The results obtained in similar shot by shot discharges are shown in Fig. 12 for 0.5, 1 and 1.5 s. An ITB-like profile in both temperature and density was formed at around 1 s. At

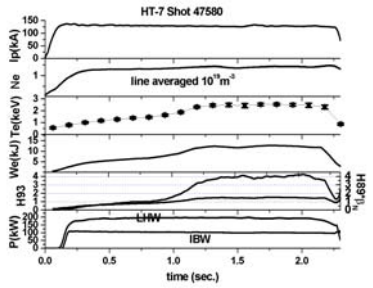

Fig. 11. High performance plasma discharge with H_{93} >1 and H_{89} β_N for about 50 τ_E.*

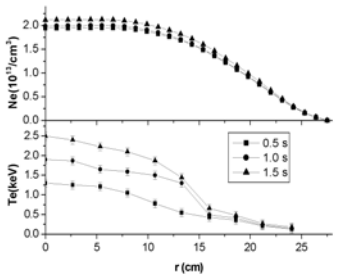

Fig. 12 Density and temperature profiles for shot 47580.

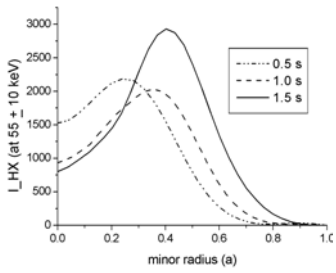

Fig. 13. HXR profiles for shot 47580.

this time, a clear enhancement of the plasma performance was initiated. The profiles of LHW driven fast electron current density evolved as shown in Fig. 13 and reached to a stable state at about 1 s. The position of the maximum fast electron current channel at 1.4 s was at nearly the same radius, where the electron temperature and density profiles had the largest gradients. This clear correlation between the location of the first maximum $n_{||}$ and HXR profiles suggests the role of the localized fast electron current density and the created plasma profiles in the plasma performance. This operation mode utilizing the synergy effect of IBW and LHCD provides a new way to obtain steady-state operation in an advanced tokamak scenario.

2. Progress of Experiments on the HL-1M Tokamak

2.1. Introduction

With more powerful auxiliary heating and some advanced fueling methods, the main plasma parameters (I_p=320 kA, B_t=2.8 T, n_e=8×10^{19} m^{-3}, T_i=1 keV) have been increased on the HL-1M (R=102 m, a=0.26 m) tokamak. In the auxiliary heating experiments with 3.5 MW total power, MHD instabilities, edge turbulence and plasma confinement have been investigated. During ECRH, suppression and excitation of the MHD instabilities have been observed with different conditions. The experimental results show that energetic electrons play an important role and that fishbone-like instability can be excited by ECRH and LHCD. In fueling experiments, it has been proved that Supersonic Molecular Beam Injection (SMBI) can enhance the penetration depth and fueling efficiency. The maximum line average electron density, which is near to the Greenwald limit, has been obtained with SMBI. During SMBI the energy confinement time increases by 10-30 % compared with conventional gas puffing. The characteristic features of the cluster appear with a high gas pressure source (more than 1.0 MPa).

2.2. Kinetic MHD Instability during ECRH in HL-1M [9]

ECRH experiments have been focused on the control of plasma pressure and current density profiles and on suppressing NTM in several tokamaks. The kinetic effect of energetic electrons on MHD modes is a relatively new phenomenon discovered recently in DIII-D[10]. Fishbone instabilities were excited when the ECR location was on the high field side near the q=1 surface， but the energetic ions from neutral beam injection also play a

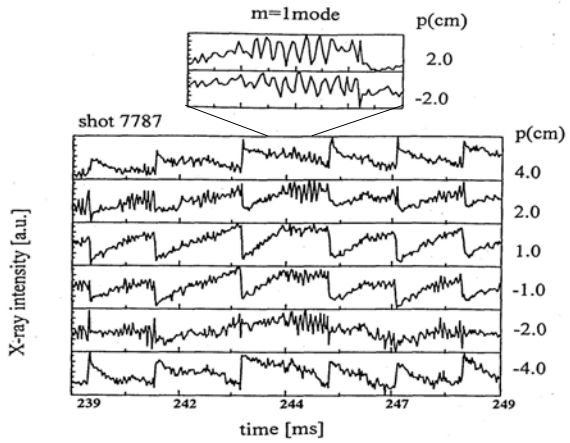

Fig. 14 Raw data of ECRH driven kinetic MHD instability.

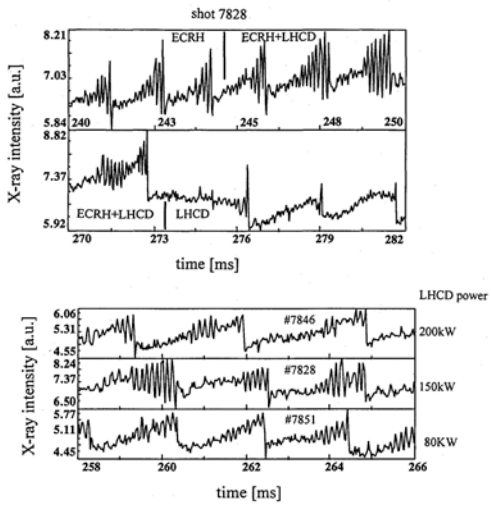

Fig. 16 a) Response of the instability to combined LHCD and ECRH. b) Response of the instability to different LHW power levels

role in the DIII-D experiment[11]. In HL-1M, we manage to excite the same instability with energetic electrons alone, i.e., there is no neutral beam injection here, and therefore, this instability is driven purely by energetic electrons.

A 75 GHz gyrotron provides ECRH power of up to 300 kW for 50 ms at the fundamental electron cyclotron resonance at B=2.68 T. Waves polarized in the ordinary mode are launched on the mid-plane from the low field side of the tokamak and propagate perpendicular to the toroidal magnetic field. Strong m/n=1/1 modes were observed during off-axis ECRH on HL-1M when the cyclotron resonance was located just outside the q=1 surface on the high field side of the magnetic axis shown as Fig.14. The m/n=1/1 mode was

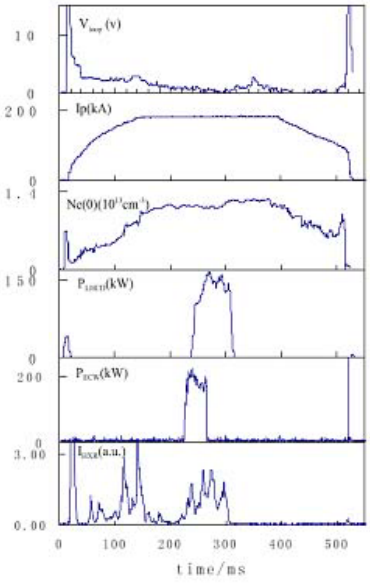

Fig. 15 A typical shot with ECRH and LHCD. (a) V_P, (b) I_P, (c) n_e, (d) LHCD power, (e) ECRH power.

a precursor that appears just before the sawtooth crash. At low ECRH power, the amplitude of the precursor is enhanced and it appears at an earlier time. The m=1 mode has a frequency of 8 kHz. The peak amplitude occurs near the q=1 surface. By varying the plasma current and the toroidal magnetic field, the ECR location was scanned repeatedly over a wide range, and excitation of the m=1 mode was observed only when the ECR location is on the high field side near the q=1 surface.

A lower-hybrid wave of 2.45 GHz with $n_{||}$ in the range of 2.0 – 3.5 was launched into the ECR heated plasma. This power spectrum should flatten the electron distribution function for electrons with parallel energy between 20 and 64 keV. The waveforms for a typical shot with combined ECRH and LHCD are shown in Fig. 15. The combined effect of ECRH and LHCD on the m/n=1/1 mode is shown in Fig. 16. The amplitude of the m/n=1 /1 mode was enhanced during two RF waves. At low LHCD

power, it takes only a few ms for the effect to appear. The fast response of the m=1 mode amplitude observed here is another indication that its excitation is due to kinetic effects from the energetic electrons rather than the local change in q (r). At high LHCD power, the response time is even shorter. A strong m=1 mode appears in every sawtooth period, and it grows to large amplitude shortly after the sawtooth crash. Figure16a shows that the m=1 mode disappears immediately after the ECRH power is turned off. This is very compelling evidence that the energetic trapped electrons with large perpendicular energy are responsible for the excitation of the instability. With the ECRH power fixed at 230 kW, the LHCD power is varied from 80 to 200 kW and its effect on the m=1 mode is depicted in Fig. 16b. It shows that the sawtooth period increases monotonically with the LHCD power, but the maximum m=1 mode amplitude appears at 150 kW of LHCD power.

2.3. High Pressure Supersonic Molecular Beam Injection in HL-1M [12]

A new fueling method, SMBI, was first proposed and demonstrated on HL-1 [13] and then used on HL-1M and HT-7 [14,15]. With the new fueling method, high densities of 8.2×10^{19} $m^{-3}$and 6.5×10^{19} m^{-3} were obtained for HL-1M and HT-7, respectively. The recent beam injection experiments have been carried out by increasing the pressure of the hydrogen gas source from 0.5 MPa to over 1.0 MPa for enlarging the characteristic dimension of the supersonic area and further enhancing the beam injection depth and fueling efficiency.

A series of interesting features have been obtained. The diagnostics show evidence of the onset of clustering, which resulted in good fueling effects. The spikes of H_α emission not only appear in the edge plasma but also in the bulk plasma, and the corresponding spikes of the VUV spectrum (OVI 103.2 nm) are detected as shown in Fig. 17. The penetration depth and injection speed of the high pressure SMB were roughly measured from the contour plot of H_α emission intensity. It is shown in Fig. 18 that the injected particles could penetrate into the core region of the plasma, and the average velocity in the plasma was estimated as about 1200 m/s, which was also verified by observation with a CCD camera located at the same cross-section of the plasma as the H_α array.

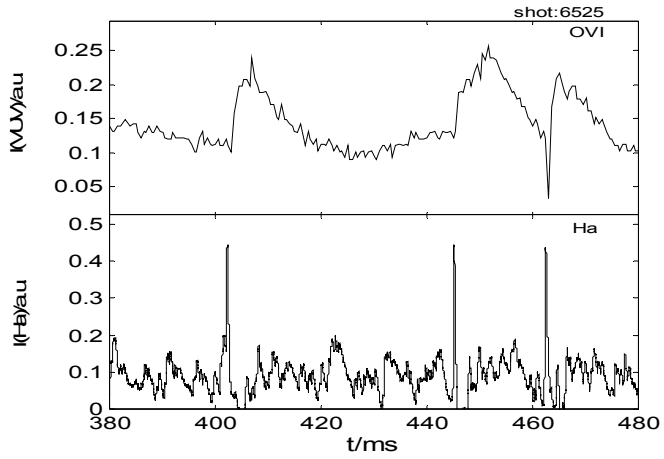

Fig. 17 Variation of H_α and OVI (103.2 nm) emission intensity after SMBI.

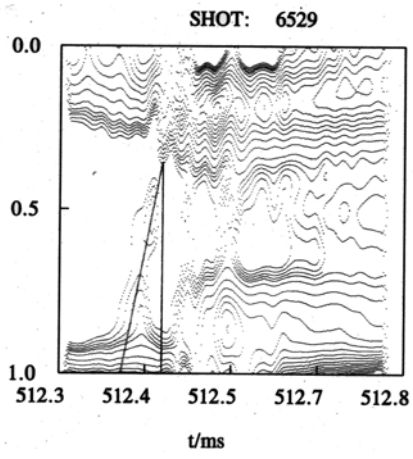

Fig. 18. SMBI velocity and penetration depth in the HL-1M plasma.

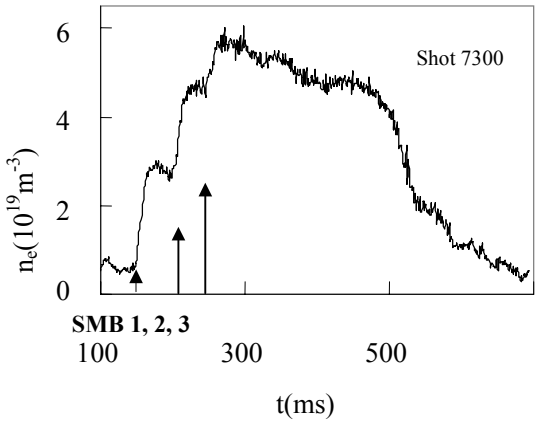

Fig. 19. Stair-shaped density increment after SMBI for three pulses.

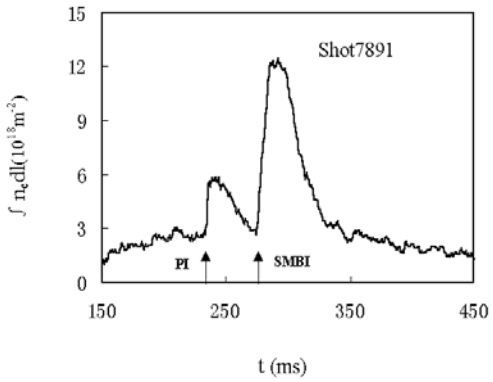

Fig. 20. Comparison of density increase rate between PI and SMBI

A stair-shaped density increment was obtained with high-pressure multi-pulse SMBI just like the density evolution behavior during the multi-pellet injection (PI) shown in Fig. 19. A comparison of fueling effects was made between high pressure SMBI and small ice PI in the same shot of an ohmic discharge during the period of the plasma current plateau on the HL-1M experiment. The increase rate of electron density for high pressure SMBI, dn_e/dt, was slightly higher than that of the small ice PI as shown in Fig. 20. The injected velocity of the pellet before it enters into the plasma is ～1000 m/s. The high pressure SMB pulse was injected at t = 280 ms with a duration of 12 ms and a source pressure of 1.15 MPa. The density increase rates for the high pressure SMBI and small PI are 1.5×10^{21} $m^{-3}s^{-1}$ and 1.2×10^{21} $m^{-3}s^{-1}$, respectively.

The reason for SMB deep penetration into the plasma at high pressure might be explained by the shielding effect. The basic shielding models have been presented [16]. The idea of this model is as follows: when the SMB is injected into the plasma and crosses the magnetic field line, the electrons interact with the neutral particles through elastic collision, excitation, dissociation and ionization processes. In this case, because the neutral particle density in the beam is larger than the density of the plasma, the electron loses most of its energy; hence, the electron slows down. This means that the electronic pile will be produced and a plasma sheath at two sides of the beam will be formed. The two sides of the beam are basically symmetric, so the plasma sheath will become an electrostatic double layer structure.

3. Summary and Conclusion

Significant progress in obtaining high performance discharges under steady state in the HT-7 superconducting tokamak has been realized since the last IAEA meeting. In relation to previous experiments, various features of non-inductive current drive, heating, profile control, fueling, MHD stabilization and edge physics have been integrated and optimized to achieved steady-state high performance discharges. HT-7 has produced a variety of discharges with the normalized performance $\beta_N*H_{89} > 1\sim4$ for a duration of several to several tens of energy confinement times with a non-inductive driven current of 50-80%.

The normalized performance indicated by the product β_N*H_{89} >3 is achieved for a duration of > $50\tau_E$. The duration at the normalized performance of H_{89} >1.5 with β_N close to unity has been extended to >$130\tau_E$. The discharges at constant H_{93} ~ 1.5 with an ELM-free edge have been sustained for a duration of longer than $50\tau_E$ in high power heated plasmas, where the maximum electron temperature is about 3 keV. A reproducible long pulse discharge with T_e ~ 1 keV and central density ~$1x10^{19}m^{-3}$can be easily obtained with a duration 10-20 seconds.

Experimental investigation on HT-7 confirms that a local synergetic interaction between lower hybrid and ion Bernstein waves can produce a well localized non-inductive current channel. The properties of IBWs in controlling temperature and density profiles can also be integrated into the LHCD plasmas not only to improve the current drive efficiency, but also to change the local electron pressure profile. This feature is particularly important because the volume of high performance plasma could be significantly extended by proper selection of plasma and wave parameter space. Operation of IBW and LHCD synergetic discharges was optimized through moving the IBW resonant layer to maximize the plasma performance and to avoid MHD activity.

Efforts have been made to achieve improved confinement discharges by using ECRH, LHCD and SMBI in the HL-1M tokamak. An interesting phenomenon has been observed during ECRH and LHCD. A strong fishbone instability driven by energetic electrons was observed during off-axis ECRH in the HL-1M tokamak. This result is a clear demonstration of the suprathermal trapped electron effect on the instability because of the absence of energetic ions in the plasma. Recently new results of SMBI experiments were obtained by increasing the gas pressure from 0.5 MPa to over 1.0 MPa. A stair-shaped density increment was obtained with high-pressure multi-pulse SMBI just like the density evolution behavior during the multipellet injection. This demonstrated the effectiveness of SMBI as a promising fueling tool for steady-state operation.

A quasi-steady-state high performance plasma has been realized. To fully understand the underlying physics, more coupling between theories, simulation and accurate experimental measurements is required. Relaxation on a scale much longer than current skin time raises new physical questions. Further optimization of the potential for long pulse discharges at integrated high performance (high H and β_N) will be the goal of the HT-7 program in the near future.

Reference

[1] Baonian Wan et al,, “PSI Issues toward Steady State Plasmas in the HT-7 Tokamak”, 15th PSI, paper I-11, May 27-31 2002, Gifu, Japan.
[2] Yanping Zhao, Baonian Wan, Jiangang Li, “Heating and Active Control of Profiles and Transport by IBW in the HT-7 Toakamak”, this conference, paper EX/P3-21.
[3] Gousheng Xu, et al., “Modification of Boundary Plasma Behavior by Ion Bernstein Wave Heating on the HT-7 Tokamak”, this conference, paper EX/P3-08.
[4] E.F. Jaeger, L.A. Berry and D.B. Batchelor, Phys. Plasmas **7** (2000), 3319.
[5] Bojiang Ding, et al., “High Confinement Plasma by Lower Hybrid Current Drive on HT-7 Superconducting Tokamak”, this conference, paper EX/P3-17.

[6] Yuejiang Shi, et al., “Fast Electron Dynamics during Lower Hybrid Current Drive Experiments in the HT-7 Tokamak”, this conference, paper EX/P3-19.
[7] Baonian Wan, et al., “Investigation of the Synergy of IBW and LHCD for Integrated High Performance Operation in the HT-7 Tokamak”, this conference, paper EX/P3-20.
[8] A. Cardinali, et al., Nucl. Fusion **42** (2002) 427.
[9] X.T. Ding, et.al “ECRH Experiments and MHD Instabilities on HL-1M”, this conference, paper EX/P4-09
[10] A.D. Turnbull et al., Phys. Rev. Lett. 74, (1995) 718.
[11] K.L. Wong et al., Phys. Rev. Lett. 85, (2000) 996.
[12] L.H. Yao et.al. “Experiments on High Pressure Supersonic Molecular Beam Injection in the HL-1M Tokamak”, this conference, paper EX/P4-08.
[13] L.H. YAO et al., 20th EPS Conference on Controlled Fusion and Plasma Physics, Lisbon, 1993, Vol. 17C(I), 303.
[14] L.H. YAO et al., Nucl. Fusion, **41,** (2001) 817**.**
[15] X. GAO et al., Nucl. Fusion, **40,** (2000) 1875**.**
[16] Shi Binren, 2001 Nuclear Fusion and Plasma Physics 21 (in Chinese) 200.